FULL PAPER

Dalton
www.rsc.org/dalton

2,2′-Bipyrimidine- and 2,3-bis(2-pyridyl)pyrazine-containing manganese(II) compounds: structural and magnetic properties

Donatella Armentano,[a] Giovanni de Munno,*[a] Francesca Guerra,[a] Juan Faus,[b] Francesc Lloret[b] and Miguel Julve*[b]

[a] *Dipartimento di Chimica Inorganica, Università degli Studi della Calabria, 87030-Arcavacata di Rende (Cosenza), Italy. E-mail: demunno@unical.it.*

[b] *Departament de Química Inorgànica/Instituto de Ciencia Molecular, Facultat de Química de la Universitat de València, Avda. Dr. Moliner 50, 46100-Burjassot (València), Spain. E-mail: miguel.julve@uv.es*

Received 9th September 2003, Accepted 10th October 2003
First published as an Advance Article on the web 29th October 2003

The preparation, crystal structures and magnetic properties of four different manganese(II) compounds of formula $[Mn(bipym)Cl_2]_n \cdot 2nH_2O$ (**1**), $[Mn_2(dpp)_2(H_2O)_2Cl_4] \cdot 2H_2O$ (**2**), $[Mn(dpp)(H_2O)_2]_n(ClO_4)_{2n} \cdot 1.5nH_2O$ (**3**) and $[Mn(dpp)(dca)_2]_n$ (**4**) [bipym = 2,2′-bipyrimidine, dpp = 2,3-bis(2-pyridyl)pyrazine and dca = dicyanamide anion] are reported. Compounds **1** and **3** are uniform chains of six-coordinated manganese(II) ions bridged by bis(bidentate) bipym (**1**) and dpp (**3**) ligands with two chloride groups (**1**) and two water molecules (**3**) in *cis* position. The electroneutrality in **3** is achieved by uncoordinated perchlorate anions. The manganese atom in **1** and **3** exhibits a distorted octahedral environment mainly due to the short bite angle at the bis(chelating) bipym [70.9(1)°] and dpp [72.6(2)°] ligands. The intrachain Mn · · · Mn separations are 6.164(1) Å in **1** and 7.289(2) Å in **3**. Complex **2** is binuclear with a pair of chlorine atoms bridging the manganese atoms in a central Mn_2Cl_2 plane, the intramolecular Mn · · · Mn separation being 3.805(2) Å. Each manganese atom in **2** is six-coordinated with two nitrogen atoms from a bidentate dpp, a water molecule and three chlorine atoms (one terminal and two bridging) building a distorted octahedral environment. Compound **4** is a rhombic layered compound where the manganese atoms of each sheet are linked by single μ-1,5-dca bridges with Mn · · · Mn separations of 6.909(1) and 7.674(1) Å. Each manganese atom in **4** is in a distorted octahedral environment, being coordinated to six nitrogen atoms, four from dca ligands and two from a bidentate dpp molecule. Magnetic susceptibility measurements for **1**–**4** in the temperature range 1.9–290 K show the occurrence of significant magnetic interactions between the local high spin manganese(II) ions which are antiferromagnetic across bridging bipym ($J = -1.19$ cm^{-1}, **1**), dpp ($J = -0.25$ cm^{-1}, **3**) and dca ($J = -0.26$ cm^{-1}, **4**) and ferromagnetic through the double-μ-chloro bridge ($J = +0.11$ cm^{-1}, **2**).

Introduction

The interest in multifunctional materials based on molecular crystals has been growing in recent years. Of the different research fields concerning this area, supramolecular chemistry, electron transfer processes, and magnetic coupling are among the most fascinating.[1–4] As far as the magnetic studies are concerned, the use of aromatic nitrogen heterocycles as bridging ligands has played a major role because of their good coordinating properties and their ability to transmit electronic effects. One of the best examples is 2,2′-bipyrimidine (bipym, **Ia**), a ligand that can adopt chelating and bis(chelating) coordination modes in its metal complexes yielding a plethora of extended magnetic systems.[5–11] Restricting ourselves to the Mn(II)–bipym family, dinuclear,[12] one-,[12c,13] two-[12a,c,14] and three-dimensional[10,14,15] homometallic compounds as well as heterobimetallic species[16] were prepared and magneto-structurally characterised. 2,3-Bis(2′-pyridyl)pyrazine (dpp, **Ib**) is a versatile polypyridyl type ligand with four nitrogen donor atoms like bipym but with a greater flexibility. The crystal structure of dpp was determined only twelve years ago[17] and its complex formation with Ru(II), Pt(II), Re(I) and Os(IV) has been the subject of several recent reports because of the spectroscopic, photochemical and photophysical properties of these dpp-containing compounds.[18] Concerning the complexes of dpp with first row transition metal ions, X-ray structures of complexes of dpp with Cu(I)[19] and Cu(II)[20] metal ions have shown that dpp can adopt not only the anticipated terminal bidentate and bridging bis-bidentate coordination modes but also the unexpected bidentate/monodentate[20e] and bidentate/bis-monodentate[19b] bridging modes. The largest magnetic interaction between two copper(II) ions separated by *ca.* 6.9 Å across bridging dpp is -1.2 cm^{-1}.

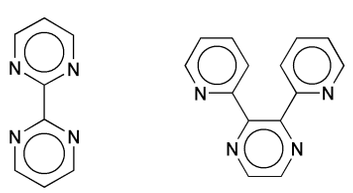

I(**a**) bipym (**b**) dpp

In the present work, we have investigated the complex formation between Mn(II), dpp and bipym in order to carry out a magneto-structural study of the resulting dpp- and bipym-containg manganese(II) polymers. The presence in the synthetic process of anions such as chloride, perchlorate and dicyanamide (dca) that can act as ligands is at the origin of the different dimensionality and magnetic properties of the isolated compounds: two uniform chains of formula $[Mn(bipym)Cl_2]_n \cdot 2nH_2O$ (**1**) and $[Mn(dpp)(H_2O)_2]_n(ClO_4)_{2n} \cdot 1.5nH_2O$ (**3**), a dinuclear complex $[Mn_2(dpp)_2(H_2O)_2Cl_4] \cdot 2H_2O$ (**2**) and a two-dimensional compound $[Mn(dpp)(dca)_2]_n$ (**4**) were obtained. Their preparation, crystal structures and magnetic properties are included here.

Experimental

CAUTION: Perchlorate salts of metal complexes with organic ligands are potentially explosive. Only small amounts of material should be prepared, and these should be handled with care.

Materials

Manganese(II) chloride tetrahydrate, manganese(II) perchlorate hexahydrate, sodium dicyanamide and bipym were purchased

DOI: 10.1039/b311007a

from commercial sources and used as received. Dpp was prepared according to the procedure of Goodwin and Lions.[21] Elemental analysis (C, H, N) were carried out by the Microanalytical Service of the Università degli Studi della Calabria (Italy).

Preparations

$[Mn(bipym)Cl_2]_n \cdot 2nH_2O$ (1). 0.1 mmol of bipym previously dissolved in 5 cm^3 of water was added to an aqueous solution (5 cm^3) of 0.1 mmol of $MnCl_2 \cdot 4H_2O$. The resulting pale yellow solution was left to evaporate at room temperature, affording irregular yellow crystals of **1** over a couple of days. The yield is about 70%. Anal. Calc. for $C_8H_{10}Cl_2MnN_4O_2$ (**1**): C, 30.02; H, 3.15; N, 17.50. Found: C, 29.95; H, 3.10; N, 17.50%.

$[Mn_2(dpp)_2(H_2O)_2Cl_4] \cdot 2H_2O$ (2). 0.1 mmol of dpp was dissolved in 3 cm^3 of ethanol. The resulting solution was added to an aqueous solution (3 cm^3) of 0.1 mmol of $MnCl_2 \cdot 4H_2O$. Yellow laminar crystals of **2** were obtained by slow evaporation of the resulting solution after a few days. The yield is about 38%. Anal. Calc. for $C_{28}H_{28}Cl_4Mn_2N_8O_4$ (**2**): C, 42.45; H, 3.56; N, 14.14. Found: C, 42.26; H, 3.48; N, 14.25%.

$[Mn(dpp)(H_2O)_2]_n(ClO_4)_{2n} \cdot 1.5nH_2O$ (3). An aqueous solution (5 cm^3) containing 0.1 mmol of $Mn(ClO_4)_2 \cdot 6H_2O$ was added to an ethanolic solution (2 cm^3) containing 0.1 mmol of dpp. Yellow needle-shaped crystals of **3** were grown after a couple of days from the resulting solution on standing at room temperature. The yield is about 70%. Anal. Calc. for $C_{14}H_{17}Cl_2MnN_4O_{11.5}$ (**3**): C, 30.50; H, 3.10; N, 10.16. Found: C, 30.15; H, 3.01; N, 10.50%.

$[Mn(dpp)(dca)_2]_n$ (4). 0.2 mmol of $Na(dca)_2$ was dissolved in the minimum amount of water and added to an aqueous solution (5 cm^3) of 0.1 mmol of $MnCl_2 \cdot 4H_2O$. The resulting solution was mixed with an ethanolic solution (2 cm^3) containing 0.1 mmol of dpp and gently warmed during 15 min. Yellow irregular crystals of **4** were separated in a couple of days by slow evaporation of the resulting solution at room temperature. The yield is about 45%. Anal. Calc. for $C_{18}H_{10}MnN_{10}$ (**4**): C, 51.32; H, 2.39; N, 33.25. Found: C, 51.15; H, 2.11; N, 33.50%.

Physical techniques

IR spectra were recorded on a Perkin Elmer 1750 FTIR spectrophotometer as KBr pellets in the 4000–400 cm^{-1} region. The magnetic susceptibilities of polycrystalline samples of the complexes were measured in the temperature range 1.9–290 K with a Quantum Design SQUID susceptometer, using an applied field of 1000 G. The complex $(NH_4)_2Mn(SO_4)_2 \cdot 6H_2O$ was used as a susceptibility standard. Diamagnetic corrections of the constituent atoms were estimated from Pascal constants[22] and found to be -185×10^{-6} (**1**), -478×10^{-6} (**2**), -268×10^{-6} (**3**) and -216×10^{-6} cm^3 mol^{-1} (**4**).

Crystallography

Crystals of dimensions 0.20 × 0.18 × 0.22 (**1**), 0.38 × 0.18 × 0.08 (**2**), 0.10 × 0.11 × 0.45 (**3**) and 0.30 × 0.20 × 0.38 mm (**4**) were mounted on a Bruker R3m/V automatic four-circle diffractometer and used for data collection. Diffraction data were collected at room temperature using graphite-monochromated Mo-Kα radiation (λ = 0.71073 Å) with the ω–2θ scan method. The unit-cell parameters were determined from least-squares refinement of the setting angles of 25 reflections in the range 2θ 15–30°. Information concerning the crystallographic data collection and structure refinements is summarized in Table 1. Examinations of a standard reflection, monitored after every 50, showed no sign of crystal deterioration. Lorentz-polarization and Ψ-scan absorption corrections[23] were applied to the intensity data. The maximum and minimum transmission factors were 0.773 and 0.732 for **1**, 0.914 and 0.670 for **2**, 0.915 and 0.687 for **3** and 0.548 and 0.515 for **4**.

All the structures were solved by standard Patterson methods through the SHELXTL NT package[24] and subsequently completed by Fourier recycling. All non-hydrogen atoms were refined anisotropically in **1**, **2** and **4**. Only Mn(1), the water oxygen atoms O(1), O(2) and O(11) and the atoms of one perchlorate anion in compound **3** have been refined anisotropically. The other perchlorate anion contains the atoms Cl(2) and O(10) which are disordered in two positions. A crystallization water molecule is disordered in **3** and the occupancy factor of the corresponding oxygen atom was set as 0.5. Hydrogen atoms of the bipym and dpp ligands were set in calculated positions and refined as riding atoms with a common fixed isotropic thermal parameter. The hydrogen atoms of the water molecules, except those of the disordered water molecules O(11) and O(12) in **3**, were located on a ΔF map and refined with restraints with an isotropic thermal parameter fixed to 0.06. In compound **2** the hydrogen atoms of O(2) have been located on a ΔF map but they were not refined. The final full-matrix least-squares refinement on F^2, minimising the function $\Sigma w(|F_o| - |F_c|)^2$, reached convergence with values of the discrepancy indices given in Table 1. For compound **4**, the calculated absolute structure Flack parameter x is 0.01(3).[25] The final geometrical calculations were carried out with the PARST program.[26] The drawings were performed using the XP utility of the SHELXTL NT system. Main interatomic bond distances and angles for **1**, **2**, **3** and **4** are listed in Tables 2, 3, 4 and 5, respectively.

CCDC reference numbers 216214 (**1**), 216215 (**2**), 216216 (**3**) and 216217 (**4**).

See http://www.rsc.org/suppdata/dt/b3/b311007a/ for crystallographic data in CIF or other electronic format.

Results and discussion

Description of the structures

$[Mn(bipym)Cl_2]_n \cdot 2nH_2O$ (1). The structure of **1** consists of neutral chains of manganese(II) ions bridged by bis(chelating) bipym, developing along the z direction. Electroneutrality is achieved by the coordination of two chlorine atoms in *cis* position. A fragment of the chain with the atom numbering is shown in Fig. 1. Neighbouring chains are connected by hydrogen bonds involving crystallization water molecules and chlorine atoms (see end of Table 2). These interactions between chains give rise to a two-dimensional network developing in the yz plane as shown in Fig. 2.

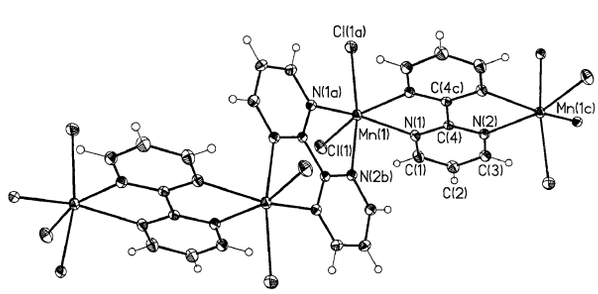

Fig. 1 Section of the chain $[Mn(bipym)Cl_2]_n$ (**1**). Thermal ellipsoids are plotted at the 30% probability level. Symmetry codes: (a) = $-x+2$, y, $-z+5/2$; (b) = x, $-y$, $z+1/2$; (c) = $-x+2$; $-y$, $-z+2$.

The manganese atom is six-coordinated: four bipym–nitrogen atoms from two bipym ligands and two chlorine atoms build a distorted octahedral environment around the metal atom. The Mn–Cl bond [2.4544(7) Å] is somewhat longer than those concerning the bipym ligand [2.306(2) and 2.339(2) Å for Mn–N(1) and Mn–N(2b), respectively]. This feature together with the the small bite angle of the bipym ligand [70.9(1)°] for

Table 1 Summary of crystal data for $[Mn(bipym)Cl_2]_n \cdot 2nH_2O$ (**1**), $[Mn_2(ddp)_2(H_2O)_2Cl_4] \cdot 2H_2O$ (**2**), $[Mn(dpp)(H_2O)_2]_n(ClO_4)_{2n} \cdot 1.5nH_2O$ (**3**) and $[Mn(dpp)(dca)_2]_n$ (**4**)

Compound	**1**	**2**	**3**	**4**
Formula	$C_8H_{10}Cl_2MnN_4O_2$	$C_{28}H_{28}Cl_4Mn_2N_8O_4$	$C_{14}H_{17}Cl_2MnN_4O_{11.5}$	$C_{18}H_{10}MnN_{10}$
M_r	320.04	792.26	551.16	421.30
Crystal system	Monoclinic	Monoclinic	Orthorhombic	Orthorhombic
Space group	*C*2/*c*	$P2_1/c$	*Pbca*	$P2_12_12_1$
a/Å	17.779(4)	9.891(2)	20.257(4)	8.1753(16)
b/Å	8.1350(16)	11.031(2)	10.050(2)	9.5485(19)
c/Å	10.181(2)	15.067(3)	21.792(4)	24.017(5)
β/°	123.87(3)	93.61(3)		
U/Å^3	1222.6(4)	1640.6(6)	4436.6(15)	1874.8(6)
Z	4	2	8	4
D_c/g cm^{-1}	1.739	1.604	1.650	1.493
F(000)	644	804	2240	852
μ(Mo-Kα)/cm^{-1}	1.511	1.143	0.902	0.732
Reflect. collcd./indep.	1465/1352	3083/2905	3922/3922	3140/2897
Reflect. obs./param.	1255/84	1361/208	1377/200	2127/263
$I > n\sigma(I)$	2	2	2	2
R_1 [a]	0.029	0.059	0.084	0.036
wR_2 [b]	0.090	0.138	0.154	0.079

[a] $R_1 = \Sigma(||F_o| - |F_c||)/\Sigma|F_o|$. [b] $wR_2 = \{\Sigma[w(F_o^2 - F_c^2)^2]/\Sigma[w(F_o^2)^2]\}^{1/2}$ and $w = 1/[\sigma^2(F_o^2) + (aP)^2 + bP]$ with $P = [F_o^2 + 2F_c^2]/3$; $a = 0.0795$ (**1**), 0.0500 (**2**), 0.0200 (**3**), 0.0410 (**4**) and $b = 1.9315$ (**1**) and 0 (**2**–**4**).

Table 2 Selected interatomic distances (Å) and angles (°) for compound **1** with esds in parentheses [a]

Mn(1)–N(1)	2.306(2)	Mn(1)–N(2b)	2.339(2)
Mn(1)–Cl(1)	2.4544(7)		
N(1)–Mn(1)–N(2c)	70.93(6)	N(1)–Mn(1)–N(1a)	153.33(8)
N(1)–Mn(1)–N(2b)	90.23(6)	N(2b)–Mn(1)–N(2c)	91.21(8)
N(1)–Mn(1)–Cl(1)	93.01(5)	N(1)–Mn(1)–Cl(1a)	104.20(5)

Hydrogen bonds [b]

A	D	H	A···D	A···H	A···H–D
Cl(1)	O(1)	H(1w)	3.289(2)	2.39(1)	157(3)
Cl(1e)	O(1)	H(2w)	3.268(2)	2.37(1)	156(2)

[a] Symmetry transformations used to generate equivalent atoms: (a) = $-x + 2$, y, $-z + 5/2$; (b) = x, $-y$, $z + 1/2$; (c) = $-x + 2$, $-y$, $-z + 2$; (e) = x, $1 - y$, $1/2 - z$. [b] A = acceptor, D = donor.

Table 3 Selected interatomic distances (Å) and angles (°) for compound **2** with esds in parentheses [a]

Mn(1)–O(1)	2.141(5)	Mn(1)–N(2)	2.302(6)
Mn(1)–N(1)	2.289(6)	Mn(1)–Cl(2)	2.412(3)
Mn(1)–Cl(1)	2.523(2)	Mn(1)–Cl(1a)	2.610(2)
O(1)–Mn(1)–N(1)	159.3(2)	O(1)–Mn(1)–N(2)	88.6(2)
N(1)–Mn(1)–N(2)	71.4(2)	O(1)–Mn(1)–Cl(2)	86.2(2)
N(1)–Mn(1)–Cl(2)	99.0(2)	N(2)–Mn(1)–Cl(2)	90.7(2)
O(1)–Mn(1)–Cl(1)	102.7(1)	N(1)–Mn(1)–Cl(1)	97.1(2)
N(2)–Mn(1)–Cl(1)	168.5(2)	Cl(2)–Mn(1)–Cl(1)	91.8(1)
O(1)–Mn(1)–Cl(1a)	89.3(2)	N(1)–Mn(1)–Cl(1a)	87.0(1)
N(2)–Mn(1)–Cl(1a)	94.1(2)	Cl(2)–Mn(1)–Cl(1a)	173.3(1)
Cl(1)–Mn(1)–Cl(1a)	84.3(1)	Mn(1)–Cl(1)–Mn(1a)	95.7(1)

Hydrogen bonds [b]

A	D	H	A···D	A···H	A···H–D
N(4b)	O(1)	H(1w)	2.805(8)	1.90	163
O(2b)	O(1)	H(2w)	2.932(6)	2.01	167
Cl(2)	O(2)	H(3w)	2.981(5)	2.07	178

[a] Symmetry transformations used to generate equivalent atoms: (a) $-x + 1$, $-y + 1$, $-z + 1$; (b) $-x + 1$, $y + 1/2$, $-z + 1/2$. [b] A = acceptor, D = donor.

Table 4 Selected interatomic distances (Å) and angles (°) for compound **3** with esds in parentheses [a]

Mn(1)–O(1)	2.131(6)	Mn(1)–O(2)	2.141(6)
Mn(1)–N(1)	2.219(7)	Mn(1)–N(2)	2.306(6)
Mn(1)–N(3a)	2.276(7)	Mn(1)–N(4a)	2.213(7)
O(1)–Mn(1)–O(2)	88.7(3)	O(2)–Mn(1)–N(4a)	96.6(3)
O(1)–Mn(1)–N(1)	96.0(3)	N(1)–Mn(1)–N(2)	72.6(2)
O(1)–Mn(1)–N(2)	88.4(2)	N(1)–Mn(1)– N(3a)	94.7(2)
O(1)–Mn(1)–N(3a)	169.3(3)	N(1)–Mn(1)–N(4a)	163.2(3)
O(1)–Mn(1)–N(4a)	96.8(3)	N(3a)–Mn(1)–N(2)	94.2(2)
O(2)–Mn(1)–N(1)	94.3(3)	N(4a)–Mn(1)–N(2)	96.9(2)
O(2)–Mn(1)–N(2)	166.4(3)	N(4a)–Mn(1)– N(3a)	72.6(2)
O(2)–Mn(1)–N(3a)	90.2(3)		

Hydrogen bonds [b]

A	D	H	A···D	A···H	A···H–D
O(12)	O(1)	H(1w)	2.93(1)	2.14(5)	139(6)
O(3)	O(1)	H(2w)	2.88(1)	2.09(5)	139(6)
O(5c)	O(2)	H(4w)	2.76(1)	1.86(3)	156(6)
O(12)	O(2)	H(3w)	2.80(1)	1.90(3)	156(6)

[a] Symmetry transformations used to generate equivalent atoms: (a) $-x + 1$, $y - 1/2$, $-z + 1/2$; (c) x, $y + 1$, z. [b] A = acceptor, D = donor.

Table 5 Selected interatomic distances (Å) and angles (°) for compound **4** with esds in parentheses [a]

Mn(1)–N(1)	2.256(3)	Mn(1)–N(2)	2.289(3)
Mn(1)–N(5)	2.160(3)	Mn(1)–N(8)	2.179(3)
Mn(1)–N(10a)	2.208(4)	Mn(1)–N(7b)	2.253(4)
N(5)–Mn(1)–N(8)	98.7(1)	N(5)–Mn(1)–N(10a)	87.1(1)
N(8)–Mn(1)–N(10a)	88.8(1)	N(5)–Mn(1)–N(7b)	96.3(1)
N(8)–Mn(1)–N(7b)	89.2(1)	N(10a)–Mn(1)–N(7b)	176.3(1)
N(5)–Mn(1)–N(1)	163.1(1)	N(8)–Mn(1)–N(1)	97.0(1)
N(10a)–Mn(1)–N(1)	86.8(1)	N(7b)–Mn(1)–N(1)	90.3(1)
N(5)–Mn(1)–N(2)	93.0(1)	N(8)–Mn(1)–N(2)	168.1(1)
N(10a)–Mn(1)–N(2)	94.0(1)	N(7b)–Mn(1)–N(2)	87.3(1)
N(1)–Mn(1)–N(2)	71.7(1)		

[a] Symmetry transformations used to generate equivalent atoms code: (a) $-x + 1$, $y - 1/2$, $-z + 1/2$; (b) $-x + 2$, $y + 1/2$, $-z + 1/2$.

N(1)–Mn(1)–N(2c)] are the main distortions of the octahedral surrounding of the manganese atom. The values of the Mn–N(bipym) and Mn–Cl bond lengths are in agreement with those observed in other bipym-[12–16] and chloro-[27] containing six-coordinated manganese(II) compounds. The best equatorial plane around the metal atom is defined by Cl(1a), N(1), N(1a) and N(2b) set of atoms, the maximum atomic deviation from the mean plane being 0.168(1) Å for N(2a). The manganese atom is 0.244(1) Å out of this plane.

The pyrimidyl rings are planar [largest deviation not greater than 0.006(1) Å from the mean planes] and the carbon–carbon

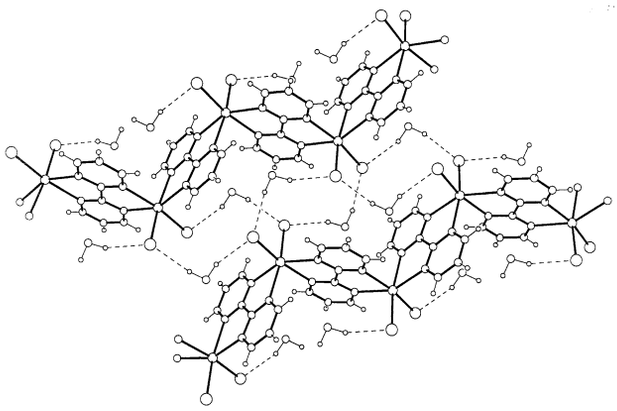

Fig. 2 Interaction between neighbouring chains in **1** creating a layer structure. Hydrogen bonds are indicated by broken lines.

and carbon–nitrogen bonds are as expected. The bipym molecule as a whole is also planar, and the metal atom is 0.034(2) Å above this plane. The dihedral angle between two adjacent bipym planes is 86.4(1)°.

The metal–metal separation across bridging bipym is 6.164(1) Å [Mn(1)···Mn(1c)], a value which lies within the range of those reported for other structurally characterised bipym-bridged manganese(II) compounds.[12–16] The shortest interchain metal–metal distance is 6.900(1) Å [Mn(1)···Mn(1d); (d) = 2 − x, 1 − y, 2 − z].

$[Mn_2(dpp)_2(H_2O)_2Cl_4]\cdot 2H_2O$ (2). The structure of **2** consists of centrosymmetric double chloro-bridged $[Mn_2(dpp)_2(H_2O)_2Cl_4]$ dimeric units (Fig. 3) and crystallization water molecules which are linked through hydrogen bonds involving the coordinated and uncoordinated water molecules plus the uncoordinated N(4) pyridyl-nitrogen atom (see end of Table 3). This extensive network of hydrogen bonds leads to a layer structure which develops in the *yz*-plane (Fig. 4).

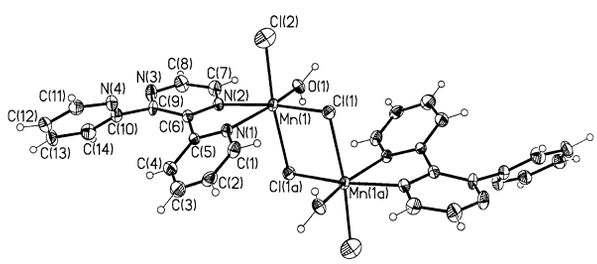

Fig. 3 Perspective view of the $[Mn_2(dpp)_2(H_2O)_2Cl_4]$ dimeric unit of **2** with the atom numbering. Thermal ellipsoids are plotted at the 30% probability level. Symmetry code: (a) = $-x+1$, $-y+1$, $-z+1$.

Each dimer contains two nearly symmetric Mn(1)–Cl(1)–Mn(1a) bridges, with Mn–Cl distances of 2.523(2) and 2.610(2) and a bridging angle of 95.68(7)°. The terminal Mn(1)–Cl(2) bond, essentially coplanar with the Mn_2Cl_2 core, is considerably shorter at 2.412(3) Å. The chloro atoms Cl(1), Cl(1a) and Cl(2), a coordinated water molecule and a bidentate dpp ligand which is bound to the manganese atom through the pyridyl N(1) and pyrazine N(2) nitrogen atoms build a distorted six-coordinated environment around the metal atom. The different nature of the ligand donor set together with the short bite of the bidentate dpp [71.4(2)° for N(1)–Mn(1)–N(2)] account for the significantly distorted octahedral surrounding of the manganese atom. The Mn–N(dpp) bond lengths [2.289(6) and 2.302(6) Å for Mn(1)–N(1) and Mn(1)–N(2), respectively] agree well with those reported for the dpp-bridged manganese(II) dimer $[Mn_2(dpp)(hfac)_4]$ [2.227(3) and 2.242(3) Å for Mn–N(pyridyl) and 2.280(3) and 2.284(3) Å for Mn–N(pyrazine)] (hfac = 1,1,1,5,5,5-hexafluoropentane-2,4-dionate).[28] The value of the Mn–O_w bond [2.141(5) Å] lies also within the range of this type

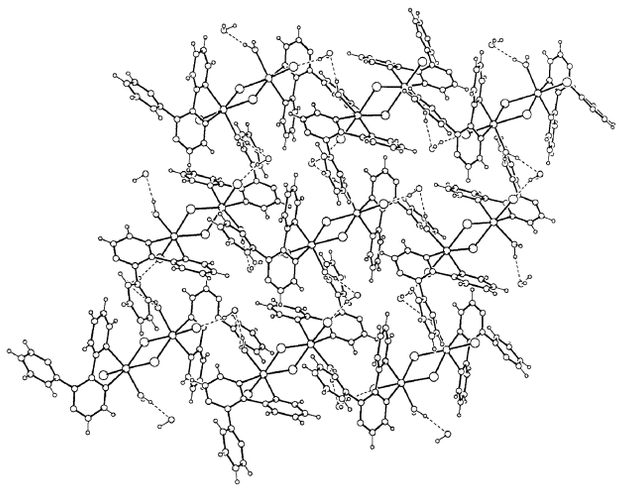

Fig. 4 Hydrogen bonding interactions (broken lines) in **2** leading to a layered structure in the *yz* plane.

of bond in similar systems.[7b,12a,29] The manganese atom is 0.053(2) Å above the best equatorial plane which is defined by the O(1), Cl(1), N(2) and N(1) set of atoms. This equatorial plane is practically orthogonal with the plane of the Mn_2Cl_2 core, the value of the dihedral angle between both planes being 89.0(1)°.

The three rings of the dpp ligand are almost planar, the maximum individual atomic deviation from mean plane being 0.039(5), 0.037(5) and 0.015(6) Å in the pyrazine, and coordinated and uncoordinated pyridyl rings, respectively. The dihedral angle between the mean planes of pyrazine and coordinated pyridyl rings is 29.7(4)°. The uncoordinated pyridyl ring is rotated by 48.6(2)° with respect to the pyrazine ring and 51.7(2)° with respect to the other pyridyl ring. Bond lengths and angles within the dpp ligand are in agreement with those observed in the free dpp.[17]

The metal–metal separation across the double chloro bridge is 3.805(2) Å [Mn(1)···Mn(1a)], a value which is much shorter than the shortest intermolecular manganese–manganese distance [6.658(2) Å for Mn(1)···Mn(1i); (i) = 1 − x, 0.5 + y, 0.5 − z].

$[Mn(dpp)(H_2O)_2]_n(ClO_4)_{2n}\cdot 1.5nH_2O$ (3). The structure of compound **3** is made up of cationic chains of dpp-bridged manganese(II) ions of formula $[Mn(dpp)(H_2O)_2]_n^{2n+}$ (Fig. 5), uncoordinated perclorate anions and crystallization water molecules which are held together by electrostatic forces, van der Waals interactions and an extensive network of hydrogen bonds involving the perchlorate oxygens and the water molecules

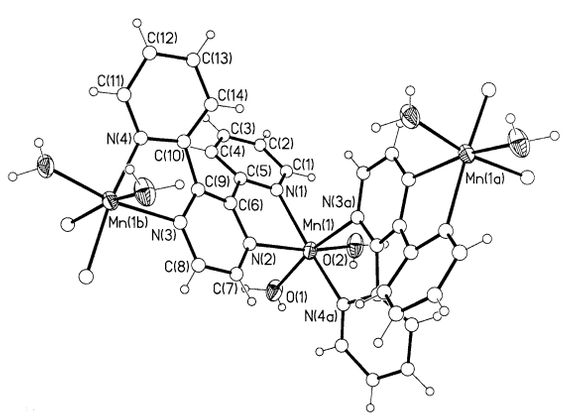

Fig. 5 Section of the cationic chain $[Mn(dpp)(H_2O)_2]_n^{2n+}$ of **3**. The perchlorate counterions and the crystallization water molecules are omitted for clarity. Thermal ellipsoids are plotted at the 30% probability level. Symmetry code: (b) = $-x$, $y-1/2$, $-z+1/2$.

(see end of Table 4). Compound **3** is isostructural with the copper(II) compounds $[Cu(dpp)(H_2O)_2]_n(X)_{2n}\cdot 2nH_2O$ where $X = ClO_4^-$ or BF_4^-.[20a,c] The prominent feature of the crystal packing in **3** is the supramolecular arrangement of the chains to create channels running through the *b*-axis (Fig. 6). These chains are located at the four corners of a rectangle, whose dimensions are 8.042(2) and 8.468(2) Å along the *a* and *c*-axes, respectively. Perchlorate anions and crystallization water molecules are hosted in the channels and they are linked to the chains through hydrogen bonds where coordination water molecules are also involved [2.88(1), 2.80(1) and 2.76(1) Å for O(1)···O(3), O(2)···O(12) and O(2)···O(5c), respectively; (c) = x, $y + 1$, z].

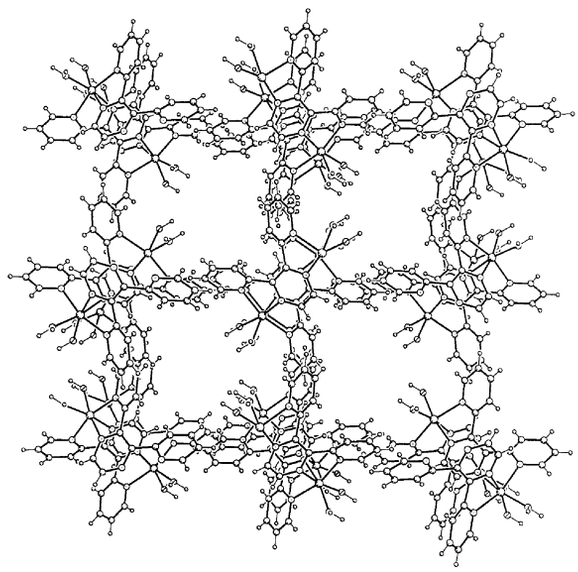

Fig. 6 A view of the packing of the chains down the *b* axis showing the large cavities which are filled by the perchlorate and the crystallization water molecules (not included for the sake of clarity).

Each manganese atom is six-coordinate MnN_4O_2: two water molecules in *cis* position [Mn(1)–O(1) 2.131(6), Mn(1)–O(2) 2.141(6) Å] and four dpp-nitrogen atoms, two pyridyl in *trans* and two pyrazine in *cis*, build a distorted octahedral environment around the metal atom. The Mn–N(pyrazine) bond lengths [average value 2.292(7) Å] are slightly longer than the Mn–N(pyridyl) ones [2.216(7) Å], as observed in **2**. The angle subtended at the manganese atom by the bridging dpp is 72.6°, a value which is somewhat larger than that observed for the bidentate dpp in **2** but practically identical to that observed for the bis-bidentate dpp in the dinuclear complex $[Mn_2(dpp)(hfac)_4]$.[28] The best equatorial plane which is defined by the O(1), N(1), N(3a) and N(4a) set of atoms, shows significant deviations from planarity [maximum atomic deviations of 0.143(4) Å for N(4a); (a) = $-x$, $0.5 + y$, $0.5 - z$], the manganese atom being 0.080(3) Å out of this mean plane.

The pyrazine ring of the dpp ligand is somewhat puckered, the maximum individual atomic deviation from mean plane being 0.068(6) Å. The pyridyl rings are less distorted: they are bent and rotated around the C(5)–C(6) and C(9)–C(10) bonds to form dihedral angles of 31.0(3) and 30.6(3)°, respectively, with the pyrazine mean plane and 56.4(3)° with each other. The N(1)–C(5)–C(6)–N(2) and N(3)–C(9)–C(10)–N(4) torsion angles are 25.0 and 28.1°, respectively, and the C(5)–C(6)–C(9)–C(10) angle is 28.9°. The dihedral angle between the mean pyrazine plane and the manganese basal plane is 86.6(2)°.

The intrachain metal–metal separation is 7.289(2) Å [Mn(1)···Mn(1a)], whereas the shortest interchain manganese–manganese distance is 8.042(2) Å [Mn(1))···Mn(1i); (i) = $-x + 1/2$, $y - 1/2$, z].

$[Mn(dpp)(dca)_2]_n$ (4). The structure of **4** is made up of parallel neutral layers of formula $[Mn(dpp)(dca)_2]$ which grow in the *xy* plane, each one consisting of an infinite array of manganese(II) ions connected by single μ-1,5-dca bridges to afford a buckled rhombic grid-like sheet (Fig. 7). The manganese–manganese separations across the end-to-end dicyanamide bridges are 6.909(1) [through [N(5)/N(7)] and 7.674(1) Å [through N(8)/N(10)], whereas the shortest interlayer metal–metal distance is 9.643(2) Å [Mn(1)···Mn(1i); (i) = $x - 1/2$, $-y + 1/2$, $-z$].

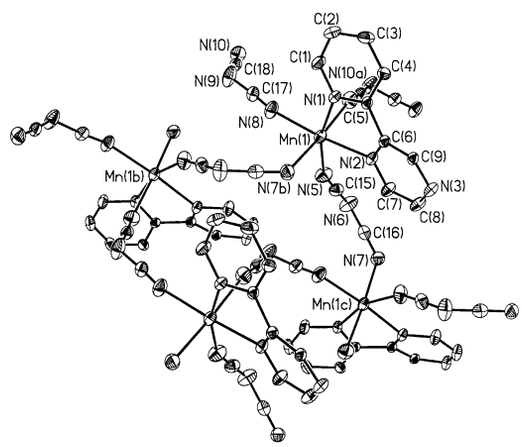

Fig. 7 A fragment of the rhombic layered structure of **4** in the *xy* plane with the atom numbering. Thermal ellipsoids are drawn at the 30% probability level. The hydrogen atoms and the uncoordinated pyridyl ring of dpp have been omitted for clarity.

Each manganese atom is in a distorted octahedral environment, being coordinated to six nitrogens atoms, four from four dca ligands and two from a dpp molecule, which acts as a terminal bidentate ligand. The reduced value of the angle subtended at the manganese atom by the chelating dpp [71.69(9)° for N(1)–Mn(1)–N(2)] can be considered the main reason for the distortion of the metal coordination sphere. The longest bond lengths [2.256(3) and 2.289(3) Å for Mn(1)–N(1) and Mn(1)–N(2), respectively] concern a pyridyl and one pyrazine nitrogen atoms from the dpp ligand, the Mn–N(dca) bonds varying in the range 2.160(3)–2.253(4) Å. The best equatorial plane around the metal atom is defined by the N(1), N(2), N(5) and N(7) set of atoms, with a maximum deviation of 0.108(2) Å for N(1). The manganese atom is shifted by 0.0295(16) Å from this mean plane.

The dca groups are bent, with C(15)–N(6)–C(16) and C(17)–N(9)–C(18) angles equal to 119.4(4) and 121.1(4)°, respectively. The dca ligands do not coordinate linearly to the manganese(II) ions: the Mn–N–C bond angles for Mn(1)–N(5)–C(15), Mn(1)–N(7b)–C(16b), Mn(1)–N(8)–C(17) and Mn(1)–N(10a)–C(18a) [symmetry codes: (a) = $-x + 1$, $y - 0.5$, $-z + 0.5$; (b) = $-x + 2$, $y + 0.5$, $-z + 0.5$] are 157.0(4) 122.6(3), 160.3(3) and 149.4(3)°, respectively. Nitrile and amide C–N distances in the dca anions vary in the ranges 1.134(4)–1.148(5) and 1.290(5)–1.307(5) Å, respectively. These values are consistent with the triple- and single-bond character and are in agreement with those observed for the end-to-end bridging mode of dca in manganese(II) compounds.[30]

As in **2**, the dpp ligand adopts a bidentate coordination mode. Its pyridyl and pyrazine coordinated rings are quasi-planar, the maximum individual atomic deviation from the mean planes being 0.044(2) Å (pyrazine) and 0.012(2) Å (pyridyl). On the other hand, the uncoordinated pyridyl ring is planar (the largest deviation from the mean plane is less than 0.004 Å). The dihedral angle between the two coordinated rings is 21.4(1)°, while the uncoordinated ring is rotated by 48.25(9)° with respect to the pyrazine and 57.9(1)° with respect to the other pyridyl ring. Finally, dpp ligands of each layer are

directed above and below the sheet in an alternating fashion. The sheets then stack in the *c* direction, with interdigitation of dpp appendages of neighbouring layers: each pyrazine ring is 3.45 Å above the uncoordinated pyridyl ring from another sheet, the angle between the mean planes being 12.8(2)° (Fig. 8).

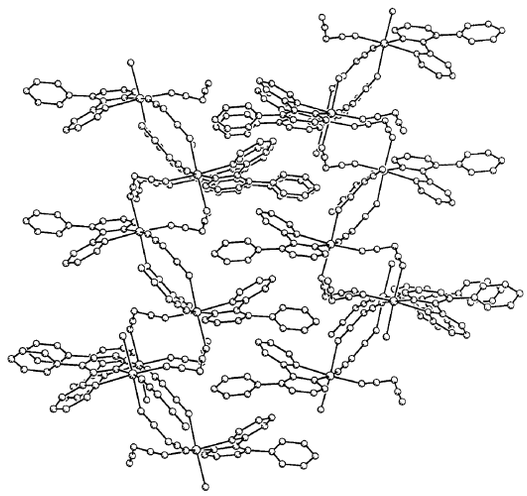

Fig. 8 A view of the arrangement of the layers of **4** down the *b* axis showing the graphite-like interactions between the pyridyl-dpp rings of adjacent layers.

Infrared spectra

The most relevant infrared absorptions of **1** concern the asymmetric doublet at 1578s and 1567w cm^{-1}, which is the signature of the presence of bis-bidentate bipym,[13,31] and the set of peaks at 3423s, br, 1637w, 834w and 673w cm^{-1}, which are associated to the crystallization water molecules.[32] The infrared spectra of **2**–**4** have in common the shift of the aromatic ring vibrations of dpp in the 1600–1350 cm^{-1} region to higher wavenumbers due to the coordination of this molecule to the manganese(II) ion.[20b–e,33] The infrared spectrum of **3** reveals the occurrence of uncoordinated perchlorate anions (1092s, br, 935w and 625m cm^{-1}).[34] Finally, the infrared spectrum of **4** shows the characteristic ν(C≡N) vibrations of the dca anion at 2409w, 2303s, 2240s, 2205s and 2178vs).[35]

Magnetic properties

The magnetic properties of the uniform manganese(II) chains **1** and **3** in the form of $\chi_M T$ *vs.* *T* plots [χ_M is the molar magnetic susceptibility] are shown in Figs. 9 and 10, respectively. Both curves are quite similar and they are characteristic of an antiferromagnetic interaction between local single-ion sextuplet states. The values of $\chi_M T$ at room temperature are *ca.* 4.28 (**1**) and 4.45 (**3**) $cm^3\ mol^{-1}$ K, and they are as expected for a magnetically isolated $S = 5/2$ spin state [the calculated value for an isolated high-spin manganese(II) ion is 4.33 $cm^3\ mol^{-1}$ K with $g = 1.99$]. Upon cooling, they decrease smoothly until 50 K and sharply at lower temperatures reaching values of 0.29 (**1**) and 1.7 $cm^3\ mol^{-1}$ K (**3**) at 1.9 K. A susceptibility maximum at 7.0 K is observed in the susceptibility curve of **1** (see insert of Fig. 9) but not in that of **3**. As **1** and **3** are uniform chains of manganese(II) ions, we have analysed their magnetic susceptibility data through the Fisher's nearest-neighbour classical Heisenberg coupling model for infinite linear chains[36] by eqn. (1) (where $u(K) = \coth K - (1/K)$ and $K = 35J/4kT$), which has been derived from the Hamiltonian (2) with $S_i = S_{i+1} = 5/2$.

$$\chi_M = \frac{35N\beta^2 g^2}{12kT}\frac{1+u(K)}{1-u(K)} \qquad (1)$$

$$\hat{H} = -J\sum_{i=1}^{n}\hat{S}_i\cdot\hat{S}_{i+1} - g\beta\sum_{i=1}^{n}H\cdot\hat{S}_i \qquad (2)$$

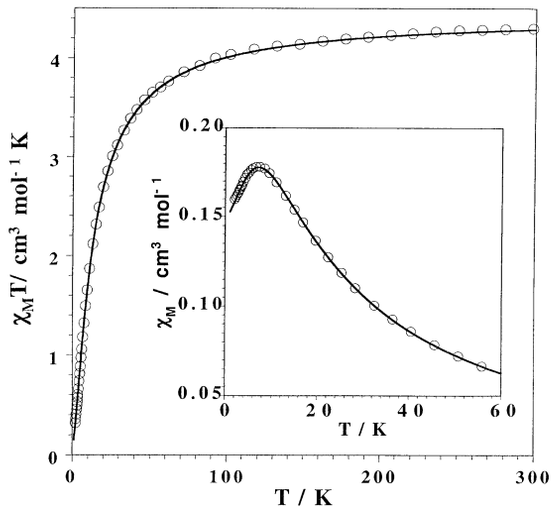

Fig. 9 $\chi_M T$ *vs.* *T* plot for complex **1**: (○) experimental data, (—) best fit curve (see text). The insert shows the χ_M *vs.* *T* plot in the vicinity of the susceptibility maximum.

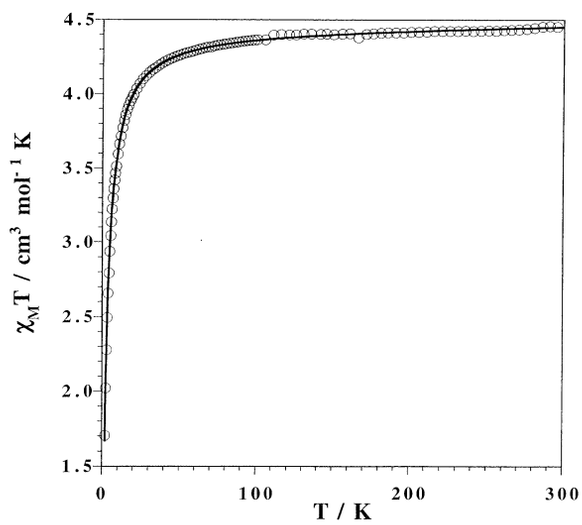

Fig. 10 $\chi_M T$ *vs.* *T* plot for complex **3**: (○) experimental data, (—) best fit curve (see text).

Least-squares fit of the susceptibility data lead to the following values: $J = -1.19\ cm^{-1}$, $g = 2.00$ and $R = 9.1 \times 10^{-5}$ (**1**) and $J = -0.25\ cm^{-1}$, $g = 2.01$ and $R = 8.0 \times 10^{-5}$; *R* is the agreement factor defined as $\Sigma_i[(\chi_M)_{obs}(i) - (\chi_M)_{calc}(i)]^2/\Sigma_i[(\chi_M)_{obs}(i)]^2$. The inclusion of an additional parameter to account for the interchain interactions in **1** and **3** was discarded because of the excellent agreement between the theoretical curves and the experimental data in the whole temperature range.

The value of the antiferromagnetic coupling between manganese(II) ions across bridging bipym in **1** ($J = -1.19\ cm^{-1}$) is in accord with those observed in previous magneto-structural studies concerning bipym-bridged manganese(II) compounds (values of *J* ranging from −0.86 to −1.20 cm^{-1}).[10,12,13,15,16] The remarkable ability of bridging bipym to mediate relatively important antiferromagnetic interactions between paramagnetic centres separated by more than 5.5 Å has been analysed previously in its complexes with other divalent first row transition metal ions such as Cu(II),[5g,j,37] Ni(II),[38] Co(II)[5e,39] and Fe(II),[5d,40] the main exchange pathway being provided by the good σ* overlap between the $d_{x^2-y^2}$ magnetic orbitals through the bipym N–C–N bridging skeleton. The magnetic coupling across bridging dpp between manganese(II) ions in **3** ($J = -0.25\ cm^{-1}$) is also antiferromagnetic and practically identical to that observed very recently in the dinuclear complex $[Mn_2(dpp)(hfac)_4]$ ($J = -0.24\ cm^{-1}$).[28] However, it lies

significantly below that observed in **1** indicating that dpp has a lower efficiency than bipym to transmit electronic interactions when these ligands adopt the bis(chelating) coordination modes. Although the σ in-plane exchange pathway is involved in **1** and **3**, the different bridging skeleton involved [two N–C–N arms (**1**) and the pyrazine ring (**3**)] causes a larger metal–metal separation in **3** [6.164(1) Å in **1** *vs.* 7.291(2) Å in **3**] and accounts for the lower efficiency of dpp.

The magnetic properties of **2** in the form of $\chi_M T$ *vs.* T plot [χ_M is the magnetic susceptibility per two Mn(II) ions] are shown in Fig. 11. $\chi_M T$ at room temperature is 8.77 $cm^3\ mol^{-1}$ K, a value which is as expected for two magnetically isolated spin sextuplets. This value remains constant when cooling to 50 K, and further, it increases to 10.4 $cm^3\ mol^{-1}$ K at 2.0 K. The profile of this $\chi_M T$ *vs.* T plot indicates the occurrence of a weak intramolecular ferromagnetic coupling between the paramagnetic Mn(II) ions. Keeping in mind the dinuclear structure of **2**, its magnetic data were fitted through the expression (3), derived from the isotropic spin Hamiltonian $\hat{H} = -J\,\hat{S}_{Mn(1)}\cdot\hat{S}_{Mn(1a)}$

$$\chi_M T = \frac{Ng^2\beta^2}{k} \times \frac{\exp(x) + 5\exp(3x) + 14\exp(6x) + 30\exp(10x) + 55\exp(15x)}{1 + 3\exp(x) + 5\exp(3x) + 7\exp(6x) + 9\exp(10x) + 11\exp(15x)} \quad (3)$$

with $x = J/kT$. Best-fit parameters are $J = +0.11$ cm^{-1}, $g = 2.00$ and $R = 1.2 \times 10^{-4}$ (R is the agreement factor defined as $\Sigma_i[(\chi_M)_{obs}(i) - (\chi_M)_{calc}(i)]^2/\Sigma_i[(\chi_M)_{obs}(i)]^2$). The ferromagnetic nature of the magnetic coupling in **2** is further confirmed by the field dependence of the magnetisation at 2.0 K (see insert of Fig. 11). The magnetization data of **2** lie between those calculated for two magnetically isolated $S = 5/2$ centres and the Brillouin function for a spin state $S = 5$. This behaviour can be attributed to an incomplete population of the predicted ground spin state $S = 5$. In fact, the population of the low lying spin state $S = 5$ in our experimental conditions is small (a plateau of $\chi_M T$ equal to 15 $cm^3\ mol^{-1}$ K taken with $g = 2.0$ is expected for the fully populated ground spin level $S = 5$ and the maximum value of $\chi_M T$ at 2.0 K is only 10.4 $cm^3\ mol^{-1}$ K).

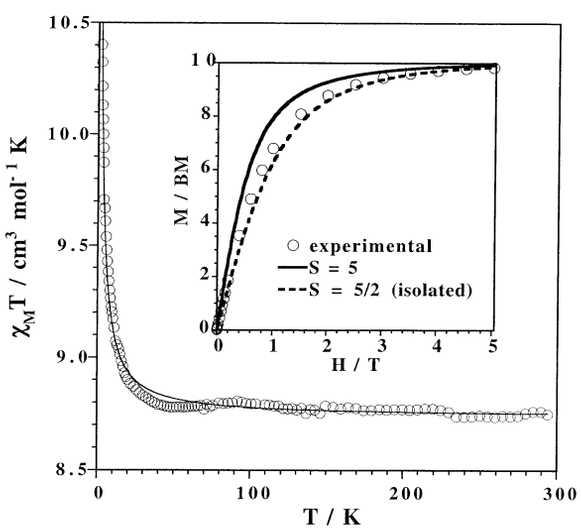

Fig. 11 $\chi_M T$ *vs.* T plot for complex **2**: (○) experimental data, (—) best fit curve (see text). The insert shows the M (○) *vs.* H plot at 2 K [the solid and broken lines are the Brillouin functions for a spin state $S = 5$ and for two magnetically isolated $S = 5/2$ centres with $g = 2.0$].

The occurrence of ferromagnetic coupling between Mn(II) ions in **2** is quite unusual. To our knowledge, ferromagnetic interactions have been observed in some Mn(II) complexes with azido,[41] diazine,[42] 4-cyanopyridine *N*-oxide[43] and Robson-type macrocyclic ligands.[44] Focusing on di-μ-chloro bridged manganese(II) dinuclear complexes, weak intramolecular antiferromagnetic interactions were observed for the six coordination of the metal atom[27a] whereas a weak ferromagnetic interaction was claimed for the complex di-μ-chloro-bis[(2,2′-biquinolyl)(chloro)manganese(II)], the metal atom being five-coordinated in this latter case.[45] The crystal structure of complex **2** contains centrosymmetric double chloro-bridged manganese(II) cationic units which are well separated from each other and where the manganese atom is six coordinated. These units can be viewed as two octahedra sharing a base-to-axial edge with parallel equatorial planes [the equatorial plane around Mn(1) is defined by the N(1)N(2)O(1)Cl(1) set of atoms and the x and y axes roughly correspond to the Mn(1)–N(1) and Mn(1)–N(2) bonds, respectively]. Under these conditions, the exchange pathway accounting for the ferromagnetic interaction concerns the dimeric unit Mn(1)Cl(1)Cl(1a)Mn(1a). Each high spin manganese(II) ion in this unit has five d-type orbitals which are singly occupied and the exchange coupling parameter J can be written as a sum of individual contributions, $J_{\mu\nu}$, involving pairs of magnetic orbitals [eqn. (4)][46]

$$J = 1/n_A n_B \sum_{\mu=1}^{n_A} \sum_{\nu=1}^{n_B} J_{\mu\nu} \quad (4)$$

where n_A and n_B are the number of unpaired electrons associated with the transition metal ions A and B ($n_A = n_B = 5$ for **2**). Positive (ferromagnetic contribution, orthogonality of the $\mu\nu$ pair) and negative (antiferromagnetic contribution, net overlap of the $\mu\nu$ pair) terms are involved in eqn. (4), the resulting sign of J being determined by a competition between them. For the planar $MnCl_2Mn$ unit of **2** and a value close to 90° at the chloro bridge, the $d_{x^2-y^2}$ [at Mn(1)] and the d_{z^2} [at Mn(1a)] magnetic orbitals (and *vice versa*) are orthogonal and consequently, the two $J_{x^2-y^2,\,z^2}$ terms are positive. By simple symmetry considerations, these terms have to be the dominant ones in **2** and a ferromagnetic coupling is predicted. As the angle at the bridging chloro atom in this compound is not far from 90° [95.7(1)° for Mn(1)–Cl(1)–Mn(1a)], this orthogonality would account for the ferromagnetic coupling observed. The paucity of magneto-structural studies with this type of compounds preclude us to go further. In order to check the correlation between the angle at the bridging chloro atom and the nature and value of magnetic coupling in Mn(II) compounds as well as to investigate the influence of additional structural factors (type of terminal ligand, type of terminal donor atoms, coordination number, *etc.*) many more examples are needed. At this respect, a recent and very nice DFT study of the exchange coupling in the wide family of halo-bridged dinuclear copper(II) complexes is particularly enlightening.[47] An important result of this study is that the presence of N-donor terminal ligands (this the case of **2**) seems to favour the ferromagnetic coupling, whereas replacement by halide anions results in antiferromagnetic behaviour.

The magnetic properties of **4** in the form of a $\chi_M T$ *vs.* T plot [χ_M is the magnetic susceptibility per Mn(II) ion] are shown in Fig. 12. $\chi_M T$ at room temperature is 4.40 $cm^3\ mol^{-1}$ K, a value which is as expected for a magnetically isolated spin sextet. Upon cooling, $\chi_M T$ is almost invariable up to 100 K and then gradually decreases to reach 0.71 $cm^3\ mol^{-1}$ K at 1.9 K. The susceptibility curve (see insert of Fig. 12) shows a maximum at 3.2 K. These features are characteristic af a weak antiferromagnetic interaction between the Mn(II) centres. Keeping in mind the two-dimensional character of **4**, the susceptibility data were fitted through Line's high-temperature series expansion for a S = 5/2 antiferromagnetic quadratic layer,[48] based on the exchange Hamiltonian $\hat{H} = -J\Sigma_{ij}\hat{S}_i\cdot\hat{S}_j$, where the sum runs over all pairs of nearest-neighbour spins i and j [eqn. (5)] in

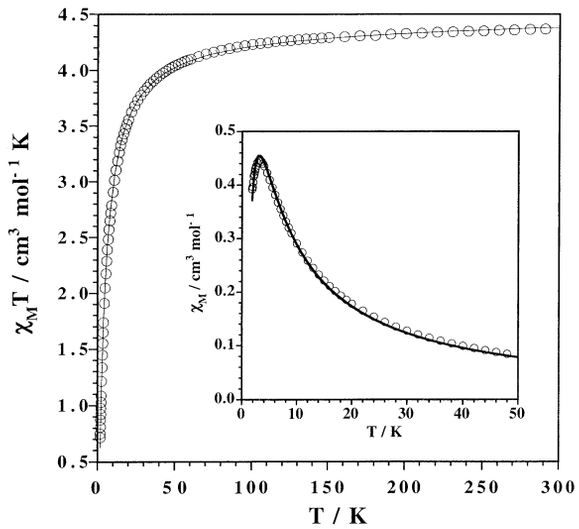

Fig. 12 $\chi_M T$ *vs.* T plot for complex **4**: (○) experimental data, (—) best fit curve (see text). The insert shows the χ_M *vs.* T plot in the vicinity of the susceptibility maximum.

which $\phi = kT/|J|S(S + 1)$, $a_1 = 4$, $a_2 = 1.448$, $a_3 = 0.228$, $a_4 = 0.262$, $a_5 = 0.119$, $a_6 = 0.017$, and N, g and β have their usual meanings.

$$Ng^2\beta^2/\chi_M|J| = 3\phi + (\Sigma a_n/\phi^{n-1}) \quad (5)$$

The best-fit parameters are $J = -0.26$ cm^{-1}, $g = 1.99$ and $R = 8.3 \times 10^{-5}$ (R is the agreement factor defined as $\Sigma_i[(\chi_M)_{obs}(i) - (\chi_M)_{calc}(i)]^2/\Sigma_i[(\chi_M)_{obs}(i)]^2$). As shown in Fig. 12, the agreement between the experimental magnetic data and the calculated values with these parameters is quite good. In this assumption we have considered that the structure of compound **4** is a quadratic layer, *i.e.* only one J value. In fact, there are two intrasheet J values in **4** (rhombic layer) but taking into account that the two exchange pathways correspond to the same μ-1,5 dicyanamide bridging mode and that the metal–metal separations through this bridge are quite large (values close to 7 Å), a similar value is reasonable for the fit.

As indicated in the reported structural description, compound **4** is made up of a pseudo-square grid arrangement of octahedral Mn(II) ions with single end-to-end dicyanamide bridges. The value of the intralayer magnetic interaction in **4** is very small ($J = -0.26$ cm^{-1}) indicating that the dicyanamide has a poor efficiency in mediating magnetic interactions when adopting the end-to-end bridging mode (metal–metal separation of *ca.* 7 Å). The value of J found for **4** agrees well with those obtained in recent reports concerning one- and two-dimensional dca-containing manganese(II) compounds where dca adopts the μ-1,5 bridging mode (values of J ranging from -0.12 to -0.34 cm^{-1}).[30c,d] Finally and for the sake of comparison, it should be noted that the magnetic coupling in the dca-bridged uniform copper(II) chain $[Cu(pyim)(H_2O)dca)]_n$ [pyim = 2-(2-pyridyl)imidazole] where single μ-1,5 dca occurs and links equatorial positions of the adjacent copper atoms is also very weak ($J = -0.35$ cm^{-1}).[49] This confirms the very low efficiency of the dca bridge (end-to-end coordination mode) to mediate magnetic interactions in its metal complexes.

Conclusions

Four new complexes of Mn(II) containing the heterocyclic ligands bipym (chain compound **1**) and dpp [dimer (**2**), chain (**3**) and sheetlike polymer (**4**)] together with coordinated chloride (**1** and **2**) and dca (**4**) and uncoordinated perchlorate (**3**) anions have been synthesized and magneto-structurally characterized. Bis(chelating) bipym (**1**) and dpp (**3**) are able to mediate significant antiferromagnetic interactions between the Mn(II) ions that they bridge, the efficiency of the former ligand being greater. Dpp acts as a bidentate ligand in **2** and **4**, two chloro atoms (**2**) and single μ-1,5-dca groups (**4**) acting as bridges. The ferromagnetically coupled dinuclear compound **2** is an interesting example of a high spin molecule which can be used as a precursor of high nuclearity homo- and heterometallic species because of the availability of two N-donor atoms of the terminal dpp ligands. The substitution of dpp by other chelating ligands and/or the replacement of the chloro bridges by other halo atoms would provide a wide family of Mn(II) polynuclear systems with ferro- and antiferromagnetic interactions which will be the basis for theoretical investigations aiming at correlating structural paramers and magnetic properties. Finally, the use of dca as coligand (**4**) allowed us to obtain a neutral layered Mn(II) compound with a significant intralayer antiferromagnetic interaction.

Acknowledgements

This work was supported by the Italian Ministero dell'Università e della Ricerca Científica e Tecnológica and the Ministerio Español de Ciencia y Tecnología through Project BQU2001-2928.

References

1 (*a*) J.-M. Lehn, *Supramolecular Chemistry*, VCH, Weinheim, 1995; (*b*) *The Crystal as a Supramolecular Entity, from Perspectives in Supramolecular Chemistry*, ed. G. R. Desiraju, Wiley, Chichester, 1996, vol. 2; (*c*) M. J. Zaworotko, *Nature*, 1997, **386**, 220; (*d*) S. C. Zimmerman, *Science*, 1997, **276**, 543.
2 (*a*) E. Coronado, J. R. Galán-Mascarós, C. J. Gomez-García, J. Ensling and P. Gütlich, *Chem. Eur. J.*, 2000, **6**, 552; (*b*) L. Martin, S. S. Turner, P. Day, P. Guionneau, J. A. K. Howard, D. E. Hibbs, M. E. Light, M. B. Hursthouse, M. Uruichi and K. Yakushi, *Inorg. Chem.*, 2001, **40**, 1363.
3 (*a*) P. Day, *Coord. Chem. Rev.*, 1999, **190–192**, 827; (*b*) J. A. McCleverty, *Acc. Chem. Res.*, 1998, **31**, 842.
4 (*a*) O. Kahn, *Molecular Magnetism*, VCH, Weinheim, Germany, 1993; (*b*) O. Kahn, *Acc. Chem. Res.*, 2000, **33**, 647.
5 (*a*) G. De Munno and M. Julve, in *Metal–Ligand Interactions. Structure and Reactivity*, ed. N. Russo and D. R. Salahub, Kluwer, Dordrecht, NATO ASI Ser. C, 1996, vol. 474, pp. 139–162; (*b*) G. De Munno, T. Poerio, G. Viau, M. Julve and F. Lloret, *Angew. Chem., Int. Ed. Engl.*, 1997, **36**, 1459; (*c*) G. De Munno, W. Ventura, G. Viau, F. Lloret, J. Faus and M. Julve, *Inorg. Chem.*, 1998, **37**, 1458; (*d*) J. Sletten, H. Daraghmeh, F. Lloret and M. Julve, *Inorg. Chim. Acta*, 1998, **279**, 127; (*e*) G. De Munno, T. Poerio, M. Julve, F. Lloret and G. Viau, *New J. Chem.*, 1998, 299; (*f*) D. Armentano, G. De Munno, F. Lloret and M. Julve, *Inorg. Chem.*, 1999, **38**, 3744; (*g*) G. De Munno, T. Poerio, M. Julve, F. Lloret, J. Faus and A. Caneschi, *J. Chem. Soc., Dalton Trans.*, 1998, 1679; (*h*) G. De Munno, D. Armentano, M. Julve, F. Lloret, R. Lescouëzec and J. Faus, *Inorg. Chem.*, 1999, **38**, 2234; (*i*) D. Armentano, G. De Munno, J. Faus, F. Lloret and M. Julve, *Inorg. Chem.*, 2001, **40**, 655; (*j*) Y. Rodríguez-Martín, J. Sanchiz, C. Ruiz-Pérez, F. Lloret and M. Julve, *Inorg. Chim. Acta*, 2001, **326**, 20; (*k*) B. Vangdal, J. Carranza, F. Lloret, M. Julve and J. Sletten, *J. Chem. Soc., Dalton Trans.*, 2002, 566.
6 (*a*) S. Decurtins, H. W. Schmalle, P. Schneuwly, L. M. Zheng, J. Ensling and A. Hauser, *Inorg. Chem.*, 1995, **34**, 5501; (*b*) S. Decurtins, H. W. Schmalle, P. Schneuwly and L. M. Zheng, *Acta Crystallogr., Sect. C*, 1996, **52**, 561.
7 (*a*) S. Kawata, S. Kitagawa, M. Enomoto, H. Kumagai and M. Katada, *Inorg. Chim. Acta*, 1998, **283**, 80; (*b*) M. K. Kabir, M. Kawahara, H. Kumagai, K. Adachi, S. Kawata, T. Ishii and K. Kitagawa, *Polyhedron*, 2001, **20**, 1417.
8 S. R. Marshall, C. D. Incarvito, J. L. Manson, A. L. Rheinhold and J. S. Miller, *Inorg. Chem.*, 2000, **39**, 1969.
9 (*a*) J. S. Sun, H. Zhao, X. Ouyang, R. Clérac, J. A. Smith, J. M. Clemente-Juan, C. Gómez-Gracía, E. Coronado and K. Dunbar, *Inorg. Chem.*, 1999, **38**, 5841; (*b*) S. Triki, F. Thétiot, J. R. Galán-Mascarós, J. Sala-Pala and K. R. Dunbar, *New J. Chem.*, 2001, **25**, 954.
10 S. Martín, M. G. Barandika, J. I. Ruiz de Larramendi, R. Cortés, M. Font-Bardía, L. Lezama, Z. E. Serna, X. Solans and T. Rojo, *Inorg. Chem.*, 2001, **40**, 3687.

11 B. Q. Ma, S. Gao, G. Su and G. X. Xu, *Angew. Chem., Int. Ed.*, 2001, **113**, 448.
12 (*a*) G. De Munno, R. Ruiz, F. Lloret, J. Faus, R. Sessoli and M. Julve, *Inorg. Chem.*, 1995, **34**, 408; (*b*) G. De Munno, G. Viau, M. Julve, F. Lloret and J. Faus, *Inorg. Chim. Acta*, 1997, **257**, 121; (*c*) R. Cortés, M. K. Urtiaga, L. Lezama, J. L. Pizarro and M. I. Arriortua and T. Rojo, *Inorg. Chem.*, 1997, **36**, 5016.
13 G. De Munno, T. Poerio, M. Julve, F. Lloret, G. Viau and A. Caneschi, *J. Chem. Soc., Dalton Trans.*, 1997, 601.
14 G. De Munno, M. Julve, G. Viau, F. Lloret, J. Faus and D. Viterbo, *Angew. Chem., Int. Ed. Engl.*, 1996, **35**, 1807.
15 J. M. Herrera, D. Armentano, G. De Munno, F. Lloret, M. Julve and M. Verdaguer, *New J. Chem.*, 2003, **27**, 128.
16 L. M. Toma, R. Lescouëzec, L. D. Toma, F. Lloret, M. Julve, J. Vaissermann and M. Andruh, *J. Chem. Soc., Dalton Trans.*, 2002, 3171.
17 N. T. Huang, W. T. Pennington and J. D. Petersen, *Acta Crystallogr., Sect. C*, 1991, **47**, 2011.
18 (*a*) V. W. W. Yam, V. W. M. Lee and K. K. Cheung, *Organometallics*, 1997, **16**, 2833; (*b*) M. B. Ferrari, G. G. Fava, G. Pelosi, G. Predieri, C. Vignali, G. Denti and S. Serroni, *Inorg. Chim. Acta*, 1998, **275–276**, 320; (*c*) J. R. Kirchhoff and K. Kirschbaum, *Polyhedron*, 1998, **17**, 4033; (*d*) Y. Y. Choi and W. T. Wong, *J. Chem. Soc., Dalton Trans.*, 1999, 331; (*e*) S. M. Scott, K. C. Gordon and A. K. Burrell, *J. Chem. Soc., Dalton Trans.*, 1999, 2669.
19 (*a*) K. T. Brooks, D. C. Finnen, J. R. Kirchhoff and A. A. Pinkerton, *Acta Crystallogr., Sect. C*, 1994, **50**, 1696; (*b*) D. J. Chesnut, A. Kusnetzow, R. R. Birge and J. Zubieta, *Inorg. Chem.*, 1999, **38**, 2663.
20 (*a*) L. W. Morgan, K. V. Goodvin, W. T. Pennington and J. D. Peterson, *Inorg. Chem.*, 1992, **31**, 1103; (*b*) J. Sletten and O. Bjorsvik, *Acta Chem. Scand.*, 1998, **52**, 770; (*c*) H. Grove, J. Sletten, M. Julve, F. Lloret and L. Lezama, *Inorg. Chim. Acta*, 2000, **310**, 217; (*d*) H. Grove, J. Sletten, M. Julve and F. Lloret, *J. Chem. Soc., Dalton Trans.*, 2001, 2487; (*e*) H. Grove, M. Julve, F. Lloret, P. E. Kruger, K. W. Törnroos and J. Sletten, *Inorg. Chim. Acta*, 2001, **325**, 115.
21 H. A. Goodwin and F. Lions, *J. Am. Chem. Soc.*, 1959, **81**, 6415.
22 A. Earnshaw, in *Introduction to Magnetochemistry*, Academic Press, London, 1968.
23 A. C. T. North, D. C. Philips and F. S. Mathews, *Acta Crystallogr., Sect. A*, 1968, **24**, 351.
24 SHELXTL NT, Version 5.10, Bruker Analytical X-ray Instruments Inc., Madison, WI, 1998.
25 H. D. Flack, *Acta Crystallogr., Sect. A*, 1983, **39**, 876.
26 M. Nardelli, *Comput. Chem.*, 1983, **7**, 95.
27 (*a*) R. D. Willett, *Acta Crystallogr., Sect. B*, 1979, **35**, 178; (*b*) P. O. Lumme and E. Lindell, *Acta Cystallogr., Sect. C*, 1988, **44**, 463; (*c*) A. G. Orpen, K. Brammer, F. H. Allen, O. Kennard, D. G. Watson and R. Taylor, *J. Chem. Soc., Dalton Trans.*, 1989, S1; (*d*) P. Sobota, J. Utko, S. Szafert, Z. Janas and T. Glowiak, *J. Chem. Soc., Dalton Trans.*, 1996, 3469; (*e*) A. Garoufis, S. Kasselouri, S. Boyatzis and C. Raptopoulou, *Polyhedron*, 1999, **18**, 1615.
28 T. Ishida, T. Kawakami, S. Mitsubori, T. Nogami, K. Yamaguchi and H. Iwamura, *J. Chem. Soc., Dalton Trans.*, 2002, 3177.
29 (*a*) J. Cano, G. De Munno, J. L. Sanz, R. Ruiz, J. Faus, F. Lloret, M. Julve and A. Caneschi, *J. Chem. Soc., Dalton Trans*, 1997, 1915; (*b*) M. Devereux, M. McCann, V. Leon, M. Geraghty, V. McKee and J. Wikaira, *Polyhedron*, 2000, **19**, 1205; (*c*) X. Zhang, D. Huang, W. Wang, C. Chen and Q. Liu, *Acta Crystallogr., Sect. C*, 2002, **58**, m268.
30 (*a*) J. L. Manson, C. D. Incarvito and J. S. Miller, *J. Chem. Soc., Dalton Trans.*, 1998, 3705; (*b*) J. L. Manson, A. M. Arif, C. D. Incarvito, L. M. Liable-Sands, A. L. Rheingold and J. S. Miller, *J. Solid State Chem.*, 1999, **145**, 369; (*c*) S. R. Batten, P. Jensen, C. J. Kepert, M. Kurmoo, B. Moubaraki, K. S. Murray and D. J. Price, *J. Chem. Soc., Dalton Trans.*, 1999, 2987; (*d*) A. Claramunt, A. Escuer, F. A. Mautner, N. Sanz and R. Vicente, *J. Chem. Soc., Dalton Trans.*, 2000, 2627; (*e*) S. R. Batten, P. Jensen, B. Moubaraki and K. S. Murray, *Chem. Commun.*, 2000, 2331; (*f*) I. Dasna, S. Golden, L. Ouahab, O. Peña, J. Guillevic and M. Fettouhi, *J. Chem. Soc., Dalton Trans.*, 2000, 129; (*g*) C. R. Kmety, Q. Huang, J. W. Lynn, R. W. Erwin, J. L. Manson, S. McCall, J. E. Crow, K. L. Stevenson, J. S. Miller and A. J. Epstein, *Phys. Rev. B*, 2000, **62**, 5576; (*h*) Z.-M. Wang, J. Luo, B.-W. Sun, C.-H. Yan, C.-S. Lkiao and S. Gao, *Acta Crystallogr., Sect. C*, 2000, **56**, e242; (*i*) J. L. Manson, J. A. Schuetler, U. Geiser, M. B. Stone and D. H. Reich, *Polyhedron*, 2001, **20**, 1423; (*j*) P. Jensen, S. R. Batten, B. Moubaraki and K. S. Murray, *J. Solid State Chem.*, 2001, **159**, 352; (*k*) P. M. van der Werff, S. R. Batten, P. Jensen, B. Moubaraki and K. S. Murray, *Inorg. Chem.*, 2001, **40**, 1718; (*l*) J. W. Raebiger, J. L. Manson, R. D. Sommer, U. Geiser, A. L. Rheinhold and J. S. Miller, *Inorg. Chem.*, 2001, **40**, 2578; (*m*) I. Dasna, S. Goleen, L. Ouahab, N. Daro and J. P. Sutter, *New J. Chem.*, 2001, **25**, 1572; (*n*) S. Dalai, P. S. Mukherjee, E. Zangrando and N. R. Chaudhuri, *New J. Chem.*, 2002, **26**, 1185; (*o*) A. Escuer, F. A. Mautner, N. Sanz and R. Vicente, *Inorg. Chim. Acta*, 2002, **340**, 163; (*p*) E. Q. Gao, S. Q. Bai, Z. M. Wang and C. H. Yan, *Dalton Trans.*, 2003, 1759; (*q*) E. Colacio, F. Lloret, I. B. Maimoun, R. Kivekas, R. Sillanpaa and J. Suárez-Varela, *Inorg. Chem.*, 2003, **42**, 2720.
31 (*a*) M. Julve, M. Verdaguer, G. De Munno, J. A. Real and G. Bruno, *Inorg. Chem.*, 1993, **32**, 795; (*b*) F. Berezovsky, A. A. Hajem, S. Triki, J. S. Pala and P. Molinie, *Inorg. Chim. Acta*, 1999, **248**, 8.
32 (*a*) K. Nakamoto, *Infrared and Raman spectra of Inorganic and Coordination Compounds*, John Wiley & Sons, New York, 1978.
33 J. G. H. Du Preez, T. I. A. Gerber and R. Jacobs, *J. Coord. Chem.*, 1994, **33**, 147.
34 M. R. Rosenthal, *J. Chem. Educ.*, 1973, **50**, 331.
35 (*a*) H. Köhler, A. Kolbe and G. Lux, *Z. Anorg. Allg. Chem.*, 1977, **103**, 428; (*b*) A. J. Civadze and H. Köhler, *Z. Anorg. Allg. Chem.*, 1984, **510**, 31; (*c*) B. Jukrens, W. Milius, P. Morys and W. Schnick, *Z. Anorg. Allg. Chem.*, 1998, **624**, 91.
36 M. E. Fisher, *Am. J. Phys.*, 1964, **32**, 343.
37 (*a*) G. De Munno, M. Julve, M. Verdaguer and G. Bruno, *Inorg. Chem.*, 1993, **32**, 2215; (*b*) G. De Munno, M. Julve, F. Lloret, J. Cano and A. Caneschi, *Inorg. Chem.*, 1995, **34**, 2048.
38 G. De Munno, M. Julve, F. Lloret and A. Derory, *J. Chem. Soc., Dalton Trans.*, 1993, 1179.
39 (*a*) G. Brewer and E. Sinn, *Inorg. Chem.*, 1985, **24**, 4580; (*b*) G. De Munno, M. Julve, F. Lloret, J. Faus and A. Caneschi, *J. Chem. Soc., Dalton Trans.*, 1994, 1175.
40 (*a*) E. Andrés, G. De Munno, M. Julve, J. A. Real and F. Lloret, *J. Chem. Soc., Dalton Trans.*, 1993, 2169; (*b*) G. De Munno, M. Julve, J. A. Real, F. Lloret and R. Scopelliti, *Inorg. Chim. Acta*, 1996, **250**, 81.
41 (*a*) R. Cortés, J. L. Pizarro, L. Lezama, M. I. Arriortua and T. Rojo, *Inorg. Chem.*, 1994, **33**, 2697; (*b*) S. Han, J. L. Manson, J. Kim and J. S. Miller, *Inorg. Chem.*, 2000, **39**, 4182.
42 Z. Xu, L. K. Thompson, D. O. Miller, H. J. Clase, J. A. Howard and A. Goeta, *Inorg. Chem.*, 1998, **37**, 3620.
43 M. Ryazanov, unpublished results.
44 D. Luneau, J. M. Savariault, P. Cassoux and J. P. Tuchagues, *J. Chem. Soc., Dalton Trans.*, 1988, 1225, and references therein.
45 E. Sinn, *J. Chem. Soc., Dalton Trans.*, 1976, 162.
46 O. Kahn in ref. 4*a*.
47 A. Rodríguez-Fortea, P. Alemany, S. Alvarez and E. Ruiz, *Inorg. Chem.*, 2002, **41**, 3769.
48 (*a*) M. E. Lines, *J. Phys. Chem. Solids*, 1970, **31**, 101; (*b*) A. Escuer, R. Vicente, M. A. S. Goher and F. A. Mautner, *J. Chem. Soc., Dalton Trans.*, 1997, 4431, and references therein.
49 J. Carranza, C. Brennan, J. Sletten, F. Lloret and M. Julve, *J. Chem. Soc., Dalton Trans.*, 2002, 3164.